Infrared Spectra and ab Initio Calculations for the $Cl^-(CH_4)_n$ ($n = 1-10$) Anion Clusters

Zoë M. Loh, Rosemary L. Wilson, Duncan A. Wild, and Evan J. Bieske*

School of Chemistry, University of Melbourne, Australia, 3010

Mark S. Gordon*

Department of Chemistry, Iowa State University, Ames, Iowa 50011, U.S.A.

Received: July 18, 2005

In an effort to elucidate their structures, mass-selected $Cl^-(CH_4)_n$ ($n = 1-10$) clusters are probed using infrared spectroscopy in the CH stretch region (2800−3100 cm^{-1}). Accompanying ab initio calculations at the MP2/6-311++G(2df,2p) level for the $n = 1-3$ clusters suggest that methane molecules prefer to attach to the chloride anion by single linear H-bonds and sit adjacent to one another. These conclusions are supported by the agreement between experimental and calculated vibrational band frequencies and intensities. Infrared spectra in the CH stretch region for $Cl^-(CH_4)_n$ clusters containing up to ten CH_4 ligands are remarkably simple, each being dominated by a single narrow peak associated with stretching motion of hydrogen-bonded CH groups. The observations are consistent with cluster structures in which at least ten equivalent methane molecules can be accommodated in the first solvation shell about a chloride anion.

1. Introduction

The study of ion−molecule complexes presents an attractively simple and direct means for exploring solvation on a microscopic level. Early studies in which the ligand-binding enthalpies were measured using high-pressure mass spectrometry (HPMS) [1] have been complemented more recently by infrared (IR) spectroscopic investigations in which the vibrational absorptions of mass-selected clusters are probed. The spectroscopic studies have focused mainly on clusters in which the solvent molecules are attached by hydrogen bonds to a negatively charged atomic or molecular core and have often been accompanied by ab initio calculations of cluster structures and vibrational frequencies and intensities. The $Cl^-(H_2O)_n$,[2,3] $Br^-(H_2O)_n$,[2] $Cl^-(C_2H_2)_n$,[4] and $Cl^-(CH_3OH)_n$[5] clusters are among the many hydrogen-bonded anion cluster systems characterized recently using IR spectroscopy. The solvation structures for these small clusters are critically dependent on the relative strengths of the anion−solvent and solvent−solvent interactions and whether the solvent molecules are able to form hydrogen-bonded networks.

In this paper, we report IR spectra for the $Cl^-(CH_4)_n$ ($n = 1-10$) clusters in an attempt to understand the manner in which a chloride anion is progressively "solvated" by methane molecules. The spectroscopic investigations are supported by ab initio calculations for the $n = 1-3$ clusters in which minimum-energy structures and vibrational frequencies are determined. Calculated CH-stretch vibrational frequencies and intensities are used to simulate IR spectra to help establish a link between vibrational spectra and cluster structures.

Previous experimental and theoretical studies of halide−methane dimers show that CH_4 prefers to attach to a halide anion by a single linear hydrogen bond forming a complex with C_{3v} symmetry.[6−8] Configurations in which the halide is attached by multiple hydrogen bonds to the edge or face of a distorted methane tetrahedron are calculated to lie somewhat higher in energy. In larger clusters, methane is expected to be a particularly simple solvent for halide anions, as CH_4 molecules do not form H-bonds with one another and because the $CH_4\cdots CH_4$ interaction is relatively isotropic and weak ($D_0 \approx$ 130 cm^{-1}).[9−12] Furthermore, as the $Cl^-\cdots CH_4$ bond is an order of magnitude stronger than the $CH_4\cdots CH_4$ bond,[7] one might expect that the CH_4 molecules will attach directly to the Cl^- anion while space permits. If this is the case, the $Cl^-(CH_4)_n$ clusters should resemble the Ar_nCl^- clusters studied using photoelectron spectroscopy by Neumark and co-workers.[13] For these species, the Ar atoms adopt positions that maximize the number of $Cl^-\cdots Ar$ and $Ar\cdots Ar$ bonds so that in the smaller clusters ($n < 6$) the Ar atoms aggregate on one side of the Cl^- ion, gradually encasing it as the number of Ar atoms increases. The $Cl^-(CH_4)_n$ clusters might be expected to adopt similar structures, because the $Ar\cdots Cl^-$ and $Cl^-\cdots CH_4$ separations are similar (3.71 and 3.72 Å, respectively) and because the equilibrium separation and binding energy of the Ar_2 dimer (3.76 Å and 100 cm^{-1}; ref 13) are comparable to those of the $(CH_4)_2$ dimer (3.9 ± 0.2 Å and 130 ± 30 cm^{-1}; refs 9−12).

2. Experimental and Theoretical Methods

Infrared spectra of the $Cl^-(CH_4)_n$ ($n = 1-10$) clusters are obtained by scanning the IR wavelength over the CH-stretch region while monitoring production of ion photofragments. Upon excitation of a CH-stretch mode, energy migrates into a weak intermolecular bond leading to its rupture and the liberation of a charged fragment. The CH-stretch transitions of $Cl^-(CH_4)_n$ ($n = 1-10$) clusters lie in the 2800−3100 cm^{-1} range and are observable following single-photon absorption, since the energy required to remove a single CH_4 unit is <1300 cm^{-1}.[14]

The apparatus consists of a tandem mass spectrometer equipped with an ion source designed to generate cooled cluster ions. The spectrum of the Cl^-CH_4 dimer was obtained using a 1:100 CH_4/Ar mixture (backing pressure 3−4 bar) seeded with traces of CCl_4 as chloride ion precursor. The lean CH_4/Ar gas

* To whom correspondence should be addressed: evanjb@unimelb.edu.au (E.J.B.), mark@si.fi.ameslab.gov (M.S.G.).

10.1021/jp053958v CCC: $30.25
Published on Web 09/03/2005

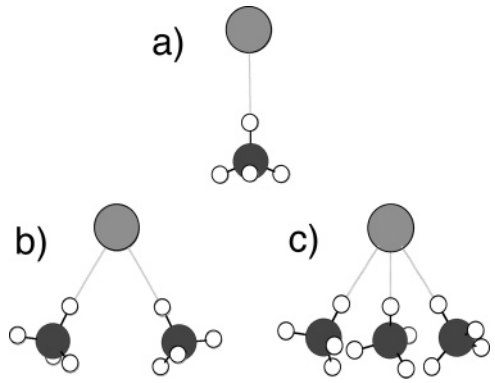

Figure 1. Minimum-energy structures for the $Cl^-(CH_4)_n$ ($n = 1-3$) complexes calculated at the MP2/6-311++G(2df,2p) level.

mixture promoted rotational cooling of the nascent Cl^-CH_4 dimer and resulted in significantly narrower vibrational bands than when pure CH_4 was used. The larger $Cl^-(CH_4)_n$ clusters ($n \geq 2$) were produced in an electron beam crossed supersonic expansion of pure CH_4 (backing pressure 3−4 bar) again seeded with traces of CCl_4. Cluster formation was optimal with a relatively small separation between the nozzle orifice and the electron impact zone, suggesting that CH_4 molecules attach to the Cl^- ion through three-body association reactions in the initial part of the expansion.

The tandem mass spectrometer comprises a primary quadrupole mass filter for selection of the parent $Cl^-(CH_4)_n$ ions, an octopole ion guide, where the ions are overlapped with the counter-propagating output of a pulsed, tuneable IR radiation source (Continuum Mirage 3000 OPO, 0.017 cm^{-1} bandwidth), and a second quadrupole mass filter tuned to the mass of the photo-fragment ions. To record IR spectra, the $(n - 1)$ photofragments were monitored for the $n = 1$ and 2 clusters, $(n - 2)$ photofragments for $n = 3$ and 4, and $(n - 3)$ photofragments for $n = 5-10$. Wavelength calibration is accomplished using a wavemeter (New Focus 7711) to measure the wavelength of the signal output from the first stage of the optical parametric oscillator, and the 532 nm output of the seeded Nd:YAG laser. Further details of the experimental setup can be found in ref 15.

Ab initio calculations for Cl^-CH_4, $Cl^-(CH_4)_2$, and $Cl^-(CH_4)_3$ were conducted at the MP2/6-311++G(2df,2p) level using the GAMESS software[16] to provide equilibrium structures, vibrational frequencies, and intensities. Only valence electrons are correlated.

3. Results and Discussion

3.1. The $Cl^-(CH_4)_n$ ($n = 1-3$) Clusters.

3.1.1. Calculated Structures. The calculated minimum-energy structures for the $n = 1-3$ complexes are shown in Figure 1. For each of the three clusters, only one stable isomer was found. As in previous theoretical studies,[6,8] the Cl^-CH_4 dimer is predicted to adopt a C_{3v} structure (Figure 1a) with the Cl^- ion attached to the methane molecule by a single, linear H-bond ($Cl^-\cdots H_b$ separation of 2.635 Å). The CH_4 subunit is slightly distorted through its interaction with the Cl^-, most notably by a very small increase in the length of the H-bonded CH group (0.005 Å). The same $Cl^-\cdots CH_4$ H-bonding motif is preserved in the $n = 2$ and 3 clusters. The minimum-energy geometry of the $Cl^-(CH_4)_2$ cluster (Figure 1b) is a V-shaped C_2 symmetry structure ($H_b-Cl^- -H_b$ bond angle, $\phi = 62°$) with the two equivalent methane ligands sitting adjacent one another. The $Cl^-(CH_4)_3$ cluster (Figure 1c) is predicted to have a pyramidal C_3 structure with three equivalent CH_4 ligands attached to the Cl^- ($H_b-Cl^-H_b$ bond angles, $\phi = 63°$). The nonbonded hydrogen atoms in the $n = 3$ clusters are interleaved in a cog-type fashion. It should be remarked that the barriers for rotating the CH_4 subunits about the axes defined by the intermolecular $Cl^-\cdots CH_4$ bonds are rather low (the calculated barrier is ~20 cm^{-1} for $n = 2$) and comparable to the CH_4 rotational constant (~5 cm^{-1}). Therefore, the methanes in the $n = 2$ and 3 clusters are expected to behave as coupled hindered rotors. In fact, it is probably misleading to think of the clusters as having well-defined structures in which the nonbonded CH groups on adjacent CH_4 molecules are in a fixed torsional relationship. Rather, even in the lower energy levels, the wave function describing the hindered rotations will extend over a range of torsional configurations.

Minor structural changes in going from $n = 1$ to 3 are consistent with progressive weakening of the intermolecular H-bonds. The most significant effect is a lengthening of the $Cl^-\cdots CH_4$ intermolecular bond (the $Cl^-\cdots H_b$ separations are 2.635, 2.653, and 2.673 Å for $n = 1$, 2, and 3, respectively). There is a corresponding slight *decrease* in the length of the H-bonded CH group (1.090, 1.089, and 1.089 Å for $n = 1$, 2, and 3). As well, the separation between the CH_4 subunits is slightly larger for $n = 3$ than for $n = 2$ (3.829 Å compared to 3.718 Å). The weakening of the H-bonds with increasing cluster size (discernible in the increasing $Cl^-\cdots CH_4$ bond lengths) is not directly reflected in a diminution in the calculated energy required to remove a single CH_4 molecule from the $n = 1-3$ clusters, which, at the MP2/6-311++G(2df,2p) level, taking vibrational zero-point energy into account, are 2.7, 2.7, and 2.9 kcal/mol, respectively. The slight upward trend in the binding energies possibly reflects the cohesive role of $CH_4\cdots CH_4$ interactions; removal of a single CH_4 molecule from the $n = 2$ and 3 clusters entails breaking, respectively, 1 or 2 methane−methane bonds as well as a $Cl^-\cdots CH_4$ bond. However, the calculated $n = 1$ and 2 binding energies are comparable with the binding enthalpies measured by HPMS (3.8 ± 0.2 and 3.5 ± 0.2 kcal/mol; ref 14).

The $Cl^-(CH_4)_2$ and $Cl^-(CH_4)_3$ structures shown in Figure 1 in which methane ligands are H-bonded to one side of the halide are favored by $CH_4\cdots CH_4$ dispersion interactions and also because dipole moment associated with the H-bonded CH groups can concertedly polarize the Cl^- anion. On the other hand, the interactions between the dipole moments induced on the methane molecules by the Cl^- charge will favor geometries in which the methanes are further apart. The interaction energy between the dipole moments induced on the two methanes in $Cl^-(CH_4)_2$ can be estimated using a classical model. Assuming the $n = 2$ geometry shown in Figure 1 ($Cl^-\cdots CH_4$ separation of 3.742 Å and $CH_4\cdots CH_4$ separation of 3.718 Å) and CH_4 polarizability of 2.663 $Å^3$ (ref 17), the induced dipole on each methane is 3.05 cm^{-1} and the induced dipole−induced dipole energy is +104 cm^{-1}. In the linear geometry, the three-body induction energy is +20 cm^{-1} (taking the $Cl^-\cdots CH_4$ separation to be 3.742 Å).

To get a sense of how easily the methane ligands are able to move around the Cl^- anion in the $Cl^-(CH_4)_2$ complex, a bending potential energy curve was calculated at the MP2/6-311++G(2df,2p) level. The $H_b-Cl^- -H_b$ angle (ϕ) was stepped in increments of 15° while all remaining coordinates were allowed to relax. The resulting potential energy curve, shown in Figure 2, has a minimum at $\phi = 62°$ and rises sharply as the two CH_4 molecules are brought closer together. In contrast, the system can move from the bent minimum to a linear configu-

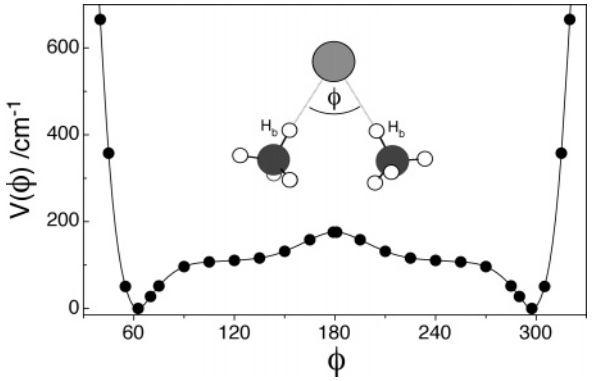

Figure 2. Potential energy curve for the lowest-frequency intermolecular bend motion of $Cl^-(CH_4)_2$. The minimum-energy configuration corresponds to $\phi = 62°$.

ration ($\phi = 180°$) at an energy cost of ~175 cm^{-1}. This energy difference is only slightly larger than the intermolecular bond energy for the $(CH_4)_2$ dimer (~130 cm^{-1}; refs 9−12).

It is worth remarking that attempts were made to locate alternative $n = 3$ structures in which at least one methane molecule is not directly H-bonded to the Cl^- anion. A second minimum was identified in which two methanes are H-bonded to the Cl^- anion while the third is attached to the backside of one of the inner-shell ligands. This extremely shallow minimum lies approximately 1100 cm^{-1} above the global minimum shown in Figure 1. It is extremely unlikely that complexes with this structure will be produced in our ion source given its much higher energy and the low barrier for isomerization into the lower-energy form (Figure 1c).

3.1.2. Calculated Vibrational Frequencies. Understanding the vibrational motions of the $Cl^-(CH_4)_n$ clusters is important, because the frequencies and intensities of the CH-stretch vibrations are the principal contact between the calculations and experiment. The vibrational modes can be separated into three distinct groups, the CH-stretch modes (around 3000 cm^{-1}), the CH_4 bend modes (around 1500 cm^{-1}), and the intermolecular modes (<200 cm^{-1}). The low-frequency intermolecular modes involve, in order of decreasing frequency, intermolecular bends (in the 130−190 cm^{-1} range for $n = 1-3$), intermolecular stretches (in the 80−120 cm^{-1} range for $n = 1-3$), torsional modes (in the 40−80 cm^{-1} range for $n = 2$ and 3), and bending motions in which the CH_4 subunits move about the Cl^- core (in the 40−50 cm^{-1} range for $n = 2$ and 3). For $n = 2$ and 3, the torsional and the lower-frequency bending motions are strongly coupled. The large-amplitude low-frequency modes are expected to be extremely anharmonic so that the ab initio harmonic frequencies probably overestimate the actual values. The torsional modes for $n = 2$ and 3, in particular, are likely to resemble hindered internal rotations about axes defined by the intermolecular H-bonds rather than harmonic vibrations. Proper description of the torsions would involve explicit consideration of coupling between the CH_4 rotors and is beyond the scope of this work.

The calculations show that the CH stretch and bend vibrational modes of methane molecules in $Cl^-(CH_4)_n$ $n = 1-3$ retain much of their free molecule character. Nonetheless, there are significant changes in their frequencies and IR intensities that should be apparent in the spectra. The evolution of the CH-stretch vibrational modes is apparent in Figure 3 where calculated CH-stretch vibrational frequencies of CH_4, Cl^-CH_4, $Cl^-(CH_4)_2$, and $Cl^-(CH_4)_3$ are plotted. When Cl^- is attached to a single CH_4, the ω_3 (t_2) stretch mode is resolved into two modes. One of these, denoted ω_3 (a_1), is IR weak and mainly

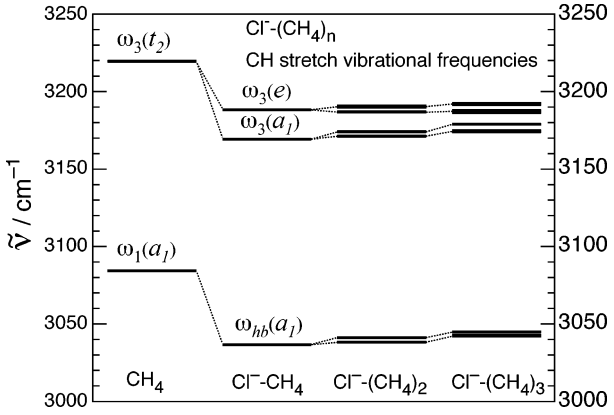

Figure 3. Calculated harmonic CH-stretch vibrational frequencies for CH_4, Cl^-CH_4, $Cl^-(CH_4)_2$, and $Cl^-(CH_4)_3$. Note the transformation of the ω_3 (t_2) mode of CH_4 to the ω_3 (a_1) and ω_3 (e) modes of Cl^-CH_4 as the symmetry is reduced to C_{3v}.

entails symmetric stretching motion of the three nonbonded CH groups. The other mode, denoted ω_3 (e), is doubly degenerate, strongly IR active, and principally involves asymmetric stretching motion of the three nonbonded CH groups. The ω_1 (a_1) symmetric stretch of CH_4 (IR inactive) is transformed into a strongly IR active vibrational mode, denoted as ω_{hb} (a_1), which principally entails stretching of the H-bonded CH group. This vibration is red-shifted from the ω_1 (a_1) mode of free CH_4. Earlier studies of the X^-CH_4 (X = F, Cl, Br) series show that the magnitude of the ω_{hb} (a_1) red-shift is directly related to the strength of the intermolecular H-bond.[7,8] As is apparent from Figure 3, the ω_3 (e) and ω_3 (a_1) modes are also red-shifted from the CH stretches of free CH_4, since they too involve some motion of the H-bonded CH group.

The CH stretch and bend modes of the $Cl^-(CH_4)_2$ and $Cl^-(CH_4)_3$ clusters shown in Figure 1 occur in groups analogous to those of the Cl^-CH_4 dimer (see Figure 3). This is because the Cl^- anion is the major influence on each CH_4 molecule, so that their local environments have effective C_{3v} symmetry, and also because vibrational coupling between the CH bonds of different CH_4 molecules is weak. The CH-stretch normal modes of the $n = 2$ complex can be described in terms of symmetric and antisymmetric combinations of equivalent vibrational motions localized on the CH_4 subunits. For example, in $Cl^-(CH_4)_2$, the ω_{hb} (a_1) vibrational motions localized on the two CH_4 subunits combine to form symmetric (3041 cm^{-1}) and antisymmetric (3038 cm^{-1}) combinations, both of which have appreciable IR intensities (3.0 and 1.1 D^2/amu.$Å^2$, respectively). A similar situation occurs for the other methane-localized vibrations of $Cl^-(CH_4)_2$ where, in each case, there are symmetric and antisymmetric combinations differing in frequency by <5 cm^{-1}. Equivalent groupings of the vibrations pertain for $Cl^-(CH_4)_3$. For example, the three local ω_{hb} (a_1) stretching motions combine to give one concerted, in-phase stretch (3045 cm^{-1}, a_1 symmetry) and a degenerate mode (3043 cm^{-1}, e symmetry).

3.1.3. Comparison Between Experimental and Simulated Spectra. Figure 4 shows the experimental IR spectra for $Cl^-(CH_4)_n$ ($n = 1-3$) clusters in the CH-stretch region together with stick spectra based on the ab initio results. In the stick spectra, the calculated harmonic CH-stretch frequencies are scaled by the factor (0.9397) required to bring the harmonic stretch frequencies for free CH_4 into line with the experimental values.

The $n = 1$ experimental spectrum has been reported previously.[7,18] Two bands are apparent, a perpendicular transition

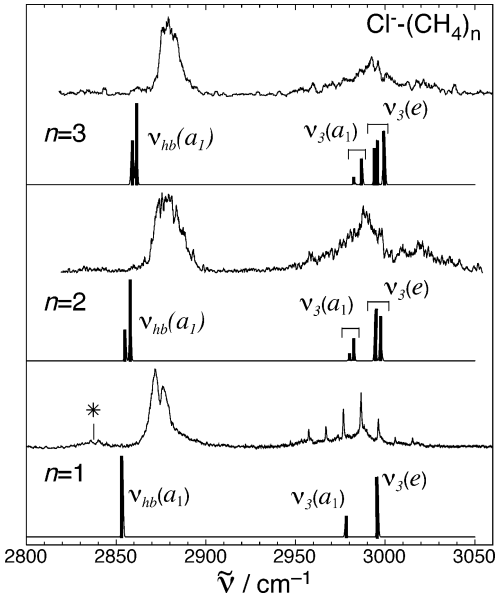

Figure 4. Infrared spectra of $Cl^-(CH_4)_n$ ($n = 1-3$) complexes in the CH-stretch region. Also shown are stick spectra representing scaled ab initio harmonic vibrational frequencies and intensities calculated at the MP2/6-311++G(2df,2p) level. See text for details.

(distinguished by prominent Q-branches spaced by ≥ 10 cm^{-1}) occurring near 2980 cm^{-1} and a parallel band lying at approximately 2875 cm^{-1} with a conspicuous band gap. By comparison with the simulated spectra, these two bands can confidently be assigned as the ν_3 (e) and ν_{hb} (a_1) transitions, respectively. The ν_3 (a_1) band, which is predicted to have an IR intensity of 0.23 that of the ν_{hb} (a_1) band is not obvious in the spectrum but may be concealed by the rather broad P and R branch structure of the ν_3 (e) band. A third much weaker band appears at 2838 cm^{-1} (asterisked in Figure 4). This band is presumably associated with the $\nu_2 + \nu_4$ combination bend level, which also appears in the IR spectrum of free CH_4 at 2845 cm^{-1}.[19]

By considering the H-bonded stretch as approximating a diatomic vibration, we estimate the temperature of the Cl^-—CH_4 complexes from the separation of the maxima in the P and R branches using $\Delta\nu_{PR}^{max} = \sqrt{8BkT/hc}$, where $B = 0.1084$ cm^{-1} from the ab initio calculations and $\Delta\nu_{PR}^{max} = 4.0 \pm 0.5$ cm^{-1} from the spectrum. This yields a rough estimate for the rotational temperature of 26 K. This value is consistent with temperature estimates derived from a fully rotationally resolved IR spectrum of the Br^-—D_2 anion produced by the same ion source where the low and high J levels were described respectively by temperatures of 25 and 85 K.[20]

Experimental spectra of $Cl^-(CH_4)_2$ and $Cl^-(CH_4)_3$ are shown in Figure 4 along with predicted stick spectra for the ab initio structures shown in Figure 1. The $n = 1-3$ spectra are similar, exhibiting relatively narrow peaks corresponding to the ν_{hb} absorptions and rather broad bands in the 2950−3050 cm^{-1} region where the ν_3 (e) and ν_3 (a_1) bands are predicted to occur. The ν_{hb} band shifts to higher frequency (a reduced red-shift) as predicted by the ab initio calculations and consistent with a weakening of the intermolecular H-bonds. The incremental shift is rather small: ~ 3 cm^{-1} for $n = 1 \rightarrow 2$ and ~ 1 cm^{-1} for $n = 2 \rightarrow 3$. Although because of the widths of the bands there is some uncertainty in the experimental incremental shifts, they are comparable with predicted shifts for the ab initio structures (3.2 and 3.5 cm^{-1}, respectively).

In the region of the ν_3 (e) and ν_3 (a_1) bands (2950−3050 cm^{-1}) the $n = 2$ and 3 spectra exhibit rather broad, noisy peaks

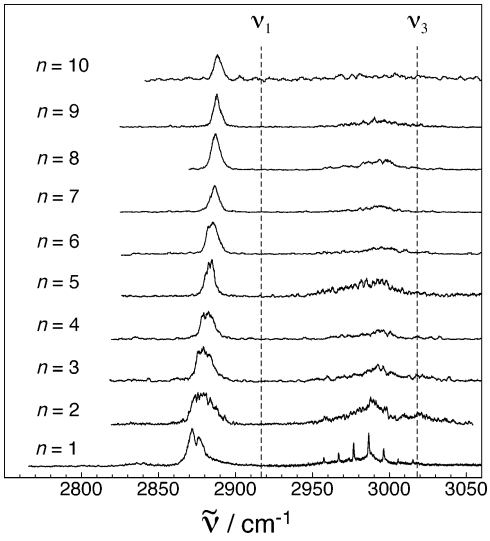

Figure 5. Infrared spectra of $Cl^-(CH_4)_n$ ($n = 1-10$) clusters in the CH-stretch region. The ν_1 (a_1) and ν_3 (t_2) stretches of free CH_4 are indicated with dashed lines.

and the sharp Q-branch structure that distinguishes the $n = 1$ ν_3 (e) band is no longer apparent. Relatively wide peaks are expected in this range, since the perpendicular ν_3 (e) bands are intrinsically broad. This situation can be contrasted with the $NH_4^+(NH_3)_n$ $n = 1-6$ clusters where the ammonia ligands are H-bonded to the central NH_4^+ and where prominent Q-branch structure is observed in the corresponding perpendicular IR bands.[21] In this case, the Q-branches correspond to $\Delta K = \pm 1$ transitions of essentially free internal NH_3 rotors. The fact that comparable Q-branch structure is not apparent in the ν_3 (e) bands of $Cl^-(CH_4)_2$ and $Cl^-CH_4)_3$ may indicate that the CH_4 rotors are hindered and coupled (because of interactions between the nonbonded H-atoms), giving rise to a rather complicated energy level patterns and spectra in the ν_3 (e) region. A second reason for the absence of Q-branch structure may be that a substantial fraction of the complexes have vibrational energy in the lower-frequency intermolecular modes. For example, the low-frequency bend vibration supported by bending potential energy curve shown in Figure 2 (ν_{imb}) is predicted to have a harmonic frequency of 46 cm^{-1}. Thus, the observed spectral bands may consist of a number of overlapping hot bands of the type ν_3 (e) + $n\nu_{imb} - n\nu_{imb}$ that are shifted slightly with respect to one another so that the Q-branches do not overlap. In the case of the $NH_4^+(NH_3)_n$ clusters, the NH_3 ligands are more restricted in the corresponding bending movement, because they are H-bonded to a relatively rigid NH_4^+ core.

3.2. Larger Clusters: $Cl^-(CH_4)_n$ ($n = 1-10$). The IR spectra of the $Cl^-(CH_4)_n$ ($n = 1-10$) clusters in the CH stretch region (2800−3100 cm^{-1}) are shown in Figure 5. Frequencies and widths of the ν_{hb} bands are listed in Table 1. Dashed lines at 2917 and 3020 cm^{-1} mark the ν_1 (a_1) and ν_3 (t_2) bands of the bare CH_4 molecule.[19] When viewed together, the $n = 1-10$ spectra in the ν_{hb} region are notable for their simplicity and regularity. The ν_{hb} band moves progressively to higher frequency (toward the ν_1 band of free CH_4) and narrows as the clusters become larger. The ν_{hb} peak for the smaller clusters ($n = 2-4$) is noticeably asymmetric with a sharp rise on the low-frequency side. Presumably, this is partially a remnant of the P-branch head that is apparent in the $n = 1$ spectrum and which is due to an increase in the rotational constants associated with a contraction in the intermolecular bond(s) accompanying excitation of the H-bonded CH stretch(es). Aside from the $n = 1$

TABLE 1: Experimental Frequencies and Bandwidths for the ν_{hb} Transitions of $Cl^-(CH_4)_n$ Clusters[a]

n	ν_{hb} (cm^{-1})	fwhm (cm^{-1})
1	2875.0 ± 2.0	12
2	2878.0 ± 2.0	18
3	2879.0 ± 2.0	12
4	2882.0 ± 2.0	10
5	2884.0 ± 1.5	7
6	2885.0 ± 1.5	8
7	2886.2 ± 1.0	7
8	2886.7 ± 1.0	7
9	2887.8 ± 1.0	5.5
10	2887.9 ± 1.0	5.5

[a] For $n = 1$, the quoted frequency corresponds to the gap between the P and R branches, whereas for the larger clusters ($n \geq 2$), the frequencies correspond to the band maxima.

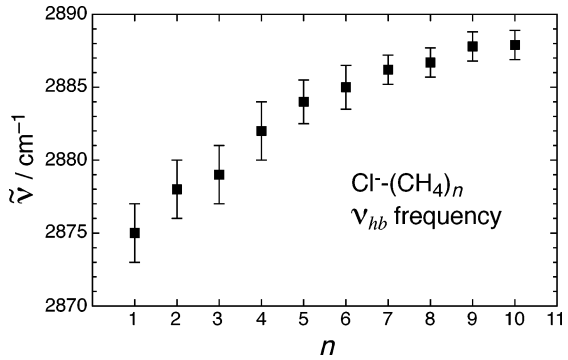

Figure 6. Experimental ν_{hb} frequencies of the $Cl^-(CH_4)_n$ ($n = 1-10$) clusters plotted vs n. For $n = 1$, the frequency corresponds to the minimum between the P and R branches, whereas for the larger clusters, the frequencies correspond to the band maxima. The error bars indicate estimated uncertainties in the band maxima frequencies.

spectrum, any apparent fine structure of the ν_{hb} peaks is not reproducible. The broad ν_3 band shifts slightly to higher frequency, gradually losing intensity until it is barely discernible for $n = 10$. The systematic migration of the ν_{hb} band to higher frequency as n increases (a diminishing red-shift) is illustrated in Figure 6 where the ν_{hb} frequency is plotted as a function of cluster size. The diminishing red-shift with increasing cluster size reflects a steady weakening of the halide−methane hydrogen bonds consistent with both the ab initio results reported in section 3.1.1, which show that the $Cl^-\cdots CH_4$ bonds lengthen with increasing cluster size and also with the measured decline of bond enthalpies for the closely related $F^-(CH_4)_{1-10}$ clusters.[14]

We turn now to a discussion of the larger clusters' structures. Given the magnitudes of the $Cl^-\cdots CH_4$ and $CH_4\cdots CH_4$ bond energies (around 1300 and 130 cm^{-1}, respectively), it seems likely that the methane molecules will tend to pack around the Cl^- anion in such as way as to maximize, first, the number of $Cl^-\cdots CH_4$ hydrogen bonds and, second, the number of $CH_4\cdots CH_4$ bonds. If the preferred $Cl^-\cdots CH_4$ and $CH_4\cdots CH_4$ separations are similar (as indicated by ab initio results for $n =$ 2 and 3), it seems likely that the clusters will adopt the compact, truncated icosahedral structures shown in Figure 7. The second to sixth CH_4 molecules are positioned in a primary five-membered ring, while the seventh to eleventh CH_4 molecules sit in a secondary five-membered ring. The secondary ring is finally capped by the twelfth CH_4 molecule. Similar icosahedral structures have been postulated for other ion clusters including Ar_nCl^-,[13] Ar_nBr^-,[22] Ar_nI^-,[22] Xe_nI^-,[23] Ar_nO^-,[24] and Ar_n-HCO^+.[25] It is worth noting that the $n = 1-3$ structures in Figure 7 match the ab initio structures described in section 3.1.1 and shown in Figure 1.

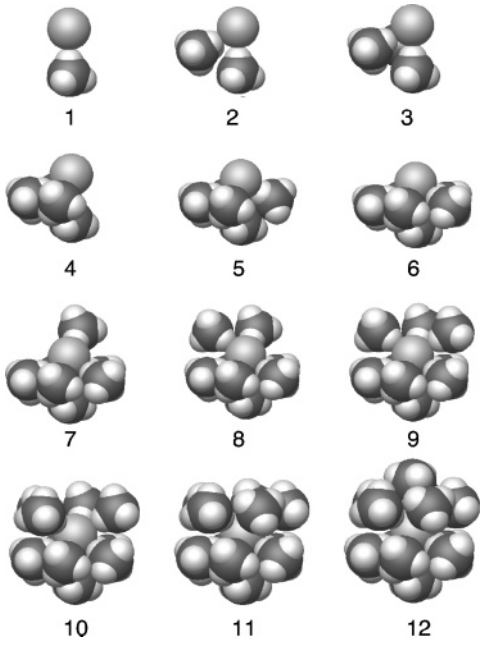

Figure 7. Postulated structures for the $Cl^-(CH_4)_n$ ($n = 1-12$) clusters.

The spectra shown in Figure 5 are consistent with the structures shown in Figure 7. The narrow ν_{hb} band in each of the $n = 1-10$ spectra shown in Figure 5 is presumably associated with CH_4 ligands directly H-bonded to the Cl^- core. The fact that the ν_{hb} band remains relatively narrow suggests that in each case the CH_4 molecules are in quite similar H-bonding environments. Initially, one might expect to see small splittings in the ν_{hb} peak reflecting the slightly different H-bonding environments of the solvent methanes. For example, the $n = 6$ cluster should exhibit two H-bonded CH-stretch bands, one corresponding to absorptions by the five CH_4 molecules in the ring and one associated with the single capping CH_4 molecule. Similarly, the $n = 7$ cluster should show five separate bands corresponding to absorptions of each of the five slightly inequivalent H-bonded CH groups in the structure shown in Figure 7. Such features are absent from the spectra; each exhibits only a single relatively narrow band in the ν_{hb} region. However, in contrast to the rigid structures shown in Figure 7, low barriers to ligand rearrangement could lead to vibrationally averaged structures having virtual equivalence of all ligands. Possibly, a combination of this effect and a small intrinsic dependence of the H-bonded CH-stretch frequency on the presence of neighboring CH_4 molecules accounts for the observation of only single ν_{hb} bands even up to $n = 10$. Possibly, spectra obtained at higher resolution than in the current study (0.02 cm^{-1}) would exhibit discernible substructure in the ν_{hb} bands.

It is worthwhile considering the possibility of cluster isomers in which methane solvent molecules are situated in a second solvent shell. Given the relative magnitude of the $Cl^-\cdots CH_4$ and $CH_4\cdots CH_4$ interaction energies, one would expect that such structures would occur for larger clusters when steric crowding prohibits CH_4 molecules from directly attaching to the Cl^-. The CH-stretch vibrations of the methane molecule in the second shell should be much closer in frequency to the ν_1 (a_1) and ν_3 (t_2) vibrations of the bare CH_4 molecule. For example, IR spectra of methane dimers and trimers in He droplets exhibit ν_3 (t_2) absorptions that are red-shifted by only a few reciprocal centimeters from those of the methane molecule, indicating that the CH_4 monomers undergo nearly free internal rotation in $(CH_4)_2$ and $(CH_4)_3$.[26] In the $Cl^-(CH_4)_n$ clusters, the ν_1 (a_1)

vibration associated with the second-shell methane would be IR weak and probably difficult to discern. On the other hand, the ν_3 (t_2) band of the second-shell ligands might be expected to exhibit Q-branches that are only slightly shifted from those of the bare methane. However, as is apparent in Figure 5, for even the larger clusters ($n = 7-10$) the broad band in the ν_3 (e) region is clearly red-shifted from the ν_3 (t_2) band of the free methane molecule. Moreover, as the clusters become larger, there is no evidence for any appreciable shift of spectral intensity toward the frequency of the bare methane ν_3 (t_2) band nor any developing Q-branch structure. For this reason, we believe that the $n = 1-10$ clusters probably adopt close-packed structures shown in Figure 7, which maximize contact between the Cl^- and CH_4 molecules. Unfortunately, the limited mass range of our apparatus prevents us from probing clusters containing more than ten methane molecules.

One of the remarkable aspects of the $n = 2-10$ spectra shown in Figure 5 is that the ν_{hb} vibrational band actually narrows as the clusters become larger. Note that the $Cl^-(CH_4)$ dimers were formed using a 1:100 CH_4/Ar mixture, leading to lower rotational temperatures (and a narrower ν_{hb} band) than the larger clusters which were formed using neat CH_4 expansion gas. The progressive reduction in ν_{hb} bandwidth, from ≥ 18 cm^{-1} for $n = 2$ to ≥ 5.5 cm^{-1} for $n = 10$, may seem surprising given that a $Cl^-(CH_4)_{10}$ cluster, for example, will possess ten ν_{hb} vibrational modes, arising from coupling between the H-bonded CH-stretch oscillators located on the ten methane subunits, each with a slightly different frequency. Clearly, the frequency spread is small. Indeed, the ab initio calculations (section 3.1.2) predict that the energy separations are less than 3 cm^{-1} for the $n = 2$ and 3 clusters. One of the major sources of band broadening is probably from overlapping hot bands associated with clusters that contain energy in the low-frequency intermolecular modes. For example, hot bands such as $\nu_{hb} + \nu_b - \nu_b$ (where ν_b is an intermolecular bend mode) will be displaced from the ν_{hb} transition because of coupling between ν_{hb} and ν_b. However, this coupling should diminish along with the strength of the H-bonds as the clusters become larger, resulting in hot bands that more closely overlap the ν_{hb} transitions of cold clusters as n increases. Similar vibrational band narrowing with increasing cluster size has been observed in spectra of $Cl^-(C_2H_2)_n$[4] and $Br^-(C_2H_2)_n$,[27] where equivalent C_2H_2 solvent molecules are bonded end-on to the halide core with no ligand−ligand H-bonding, and also in the Ar_n-HCO^+ ($n = 1-13$) clusters.[25]

4. Conclusions

In summary, ab initio calculations predict that the $Cl^-(CH_4)_n$ $n = 1-3$ clusters have structures in which equivalent methane subunits are attached to the Cl^- core by single, linear H-bonds. These structures are consistent with the experimental mid-IR spectra which each contain two bands, the lower-frequency one of which is associated with the H-bonded CH-stretch vibrations of the CH_4 subunits, while the higher-frequency band is associated with asymmetric CH-stretch vibrations of the non-bonded CH groups. Spectra of clusters containing up to ten CH_4 molecules remain relatively simple, featuring just two bands, consistent with the first solvation shell accommodating *at least* ten methane ligands.

There are several avenues for future work. Ab initio calculations for clusters containing more than three methane molecules should shed light on whether the $Cl^-(CH_4)_n$ clusters adopt the compact icosahedron-based structures postulated in this work. Complementary experimental information may also be obtainable through HPMS measurements of association enthalpies and entropies for larger $Cl^-(CH_4)_n$ clusters. Last, it would be interesting to employ IR spectroscopy to investigate larger clusters in an effort to determine how many methane molecules can be accommodated in the first solvation shell. Methane molecules sited in the second shell should exhibit ν_1 (a_1) and ν_3 (e) absorptions that are much closer to the bands of free CH_4.

Acknowledgment. We are grateful to the Australian Research Council and the University of Melbourne for financial support. We thank Prof. J. M. Lisy for helpful discussions. M.S.G. acknowledges an International Travel Grant from the National Science Foundation and a Senior Fulbright Fellowship that made this collaboration possible. The calculations were supported by a grant from the Air Force Office of Scientific Research and by a grant of computer time from the High Performance Computing Modernization Program (HPCMP) of the Department of Defense.

References and Notes

(1) Castleman, A. W.; Keesee, R. G. *Chem. Rev.* **1986**, *86*, 589.

(2) Ayotte, P.; Weddle, G. H.; Johnson, M. A. *J. Chem. Phys.* **1999**, *110*, 7129.

(3) Choi, J.-H.; Kuwata, K. T.; Cao, Y.-B.; Okumura, M. *J. Phys. Chem. A* **1998**, *102*, 503.

(4) Weiser, P. S.; Wild, D. A.; Bieske, E. J. *J. Chem. Phys.* **1999**, *110*, 9443.

(5) Cabarcos, O. M.; Weinheimer, C. J.; Martinez, T. J.; Lisy, J. M. *J. Chem. Phys.* **1999**, *110*, 9516.

(6) Novoa, J. J.; Whangbo, M. H. *Chem. Phys. Lett.* **1991**, *180*, 241.

(7) Wild, D. A.; Loh, Z. M.; Wolynec, P. P.; Weiser, P. S.; Bieske, E. *J. Chem. Phys. Lett.* **2000**, *332*, 531.

(8) Wild, D. A.; Loh, Z. M.; Bieske, E. J. *Int. J. Mass. Spectrom.* **2002**, *220*, 273.

(9) Sherwood, A. E.; Prausnitz, J. M. *J. Chem. Phys.* **1964**, *41*, 429.

(10) Matthews, G. P.; Smith, E. B. *Mol. Phys.* **1976**, *32*, 1719.

(11) Szczesniak, M. M.; Chalasinski, G.; Cybulski, S. M.; Scheiner, S. *J. Chem. Phys.* **1990**, *93*, 4243.

(12) Tsuzuki, S.; Uchimaru, T.; Tanabe, K. *Chem. Phys. Lett.* **1998**, *287*, 327.

(13) Lenzer, T.; Yourshaw, I.; Furlanetto, M. R.; Pivonka, N. L.; Neumark, D. M. *J. Chem. Phys.* **2001**, *115*, 3578.

(14) Hiraoka, K.; Mizuno, T.; Iino, T.; Eguchi, D.; Yamabe, S. *J. Phys. Chem. A* **2001**, *105*, 4887.

(15) Weiser, P. S.; Wild, D. A.; Bieske, E. *J. Chem. Phys. Lett.* **1999**, *299*, 303.

(16) Schmidt, M. W.; Baldridge, K. K.; Boatz, J. A.; Elbert, S. T.; Gordon, M. S.; Jensen, J. H.; Koseki, S.; Matsunaga, N.; Nguyen, K. A.; Su, S. J.; Windus, T. L.; Dupuis, M.; Montgomery, J. A. *J. Comput. Chem.* **1993**, *14*, 1347.

(17) Buckingham, A. D.; Orr, B. J. *Trans. Faraday Soc.* **1969**, *65*, 673.

(18) Loh, Z. M.; Wilson, R. L.; Wild, D. A.; Bieske, E. J.; Gordon, M. S. *Aust. J. Chem.* **2004**, *57*, 1157.

(19) Toth, R. A.; Brown, L. R.; Hunt, R. H.; Rothman, L. S. *Appl. Opt.* **1981**, *20*, 932.

(20) Wild, D. A.; Weiser, P. S.; Bieske, E. J. *J. Chem. Phys.* **2001**, *115*, 6394.

(21) Price, J. M.; Crofton, M. W.; Lee, Y. T. *J. Chem. Phys.* **1989**, *91*, 2749.

(22) Yourshaw, I.; Zhao, Y.; Neumark, D. M. *J. Chem. Phys.* **1996**, *105*, 351.

(23) Lenzer, T.; Furlanetto, M. R.; Pivonka, N. L.; Neumark, D. M. *J. Chem. Phys.* **1999**, *110*, 6714.

(24) Arnold, S. T.; Hendricks, J. H.; Bowen, K. H. *J. Chem. Phys.* **1995**, *102*, 39.

(25) Nizkorodov, S. A.; Dopfer, O.; Ruchti, T.; Meuwly, M.; Maier, J. P.; Bieske, E. J. *J. Phys. Chem.* **1995**, *99*, 17118.

(26) Nauta, K.; Miller, R. E. *Chem. Phys. Lett.* **2001**, *350*, 225.

(27) Wild, D. A.; Milley, P. J.; Loh, Z. M.; Weiser, P. S.; Bieske, E. *J. Chem. Phys. Lett.* **2000**, *323*, 49.